ResearchGate

See discussions, stats, and author profiles for this publication at:
https://www.researchgate.net/publication/221955656

Global synchronization in two-dimensional lattices of discrete Belousov–Zhabotinsky oscillators

ARTICLE *in* PHYSICA D NONLINEAR PHENOMENA · JUNE 2005

Impact Factor: 1.64 · DOI: 10.1016/j.physd.2005.01.007

CITATIONS
20

READS
31

3 AUTHORS, INCLUDING:

Shoichi Kai
Kyushu University

228 PUBLICATIONS **2,511** CITATIONS

SEE PROFILE

All in-text references underlined in blue are linked to publications on ResearchGate, letting you access and read them immediately.

Available from: Shoichi Kai
Retrieved on: 23 January 2016

Available online at www.sciencedirect.com
SCIENCE DIRECT®
Physica D 205 (2005) 80–86
PHYSICA D
www.elsevier.com/locate/physd

Global synchronization in two-dimensional lattices of discrete Belousov–Zhabotinsky oscillators

Hirokazu Fukuda[a,*], Hiroki Morimura[b], Shoichi Kai[a,c]

[a] *Department of Applied Quantum Physics and Nuclear Engineering, Faculty of Engineering, Kyushu University, Fukuoka 812-8581, Japan*
[b] *Department of Applied Quantum Physics and Nuclear Engineering, Graduate School of Engineering, Kyushu University, Fukuoka 812-8581, Japan*
[c] *Department of Systems Life Sciences, Graduate School of Systems Life Sciences, Kyushu University, Fukuoka 812-8581, Japan*

Available online 10 February 2005

Abstract

Macroscopic synchronization was investigated experimentally in the Belousov–Zhabotinsky reaction with a two-dimensional lattice arrangement of coupled chemical oscillators. The natural frequency of each oscillator was distributed randomly and the spacing distance d between beads was varied, where the coupling strength between two oscillators was controlled by changing d. At small d beyond a certain critical value, the oscillators synchronized spontaneously with each other. Global synchronization in the lattice was described as a function of d. The critical coupling strength for global synchronization depends on the total number of oscillators. When noisy light was applied uniformly to whole oscillators, the order of synchronization was maximized at optimal noise intensity: noise synchronization was observed.
© 2005 Elsevier B.V. All rights reserved.

Keywords: Coupled oscillators; Entrainment; Noise synchronization; Belousov–Zhabotinsky reaction

1. Introduction

The phenomenon of synchronization in a large number of coupled nonlinear oscillators has been studied in physical [1–12], chemical [13,14], and biological systems [15,16]. Populations of coupled oscillators may synchronize spontaneously to a common frequency in spite of differences in their natural frequencies. The onset of macroscopic synchronization in populations has been investigated using a simple model based on a phase description of individual oscillators [2,3]. Theoretical and numerical results predict a transition, at a certain coupling constant, from an individual oscillation to a coherent one. In particular, the transition to global synchronization in a spatially distributed oscillator system (SDOS) has attracted wide attention [4–

* Corresponding author.
E-mail addresses: fukuda@athena.ap.kyushu-u.ac.jp (H. Fukuda); kaitap@mbox.nc.kyushu-u.ac.jp (S. Kai).

0167-2789/$ – see front matter © 2005 Elsevier B.V. All rights reserved.
doi:10.1016/j.physd.2005.01.007

10] because the formation and mergence of synchronization clusters with interesting dynamics can be observed.

Experimental studies of spatially distributed and coupled oscillator systems have been performed extensively using the Belousov–Zhabotinsky (BZ) reaction. For example, spatiotemporal patterns, e.g., target and spiral patterns, were observed in a spatially continuous BZ system [17–19]. Their dynamic features have already been explained well [2]. The BZ reaction in SDOS has also been studied using cation-exchange beads, which absorbed the catalyst ions [20–26]. When the beads are immersed in the catalyst-free BZ solution with proper concentrations, the BZ reaction occurs only on the surface of individual beads. Thereupon, individual beads become localized oscillators that exhibit a stable limit-cycle oscillation. In general, the SDOS may have four different characteristic scales: the distance between the nearest-neighbor oscillators, the coupling length via diffusion, the characteristic length of the generated pattern field, and the system size [27]. In the bead oscillator system, there is one more characteristic scale: the radius of the oscillator. Depending on relative magnitudes among these scales, local, global and non-local couplings are possible. Therefore, the bead oscillator system may also show a variety of dynamics such as global and non-local coupling systems, as suggested by Kuramoto [28–30]. By careful choices of the concentration for chemicals and scales in the bead oscillator system, a non-locality of the coupling could be realized. Very recently, there are reports that noise enhances the synchronization in coupled bead oscillators at an optimal noise intensity [25,26]. Therefore, noise may also play an important role in influencing interactions and characteristic scales. However, that role has not been clarified experimentally yet in a large number of BZ oscillators.

This study investigated global synchronization in SDOS experimentally using cation-exchange beads absorbing catalyst ions and the catalyst-free BZ solution as the discrete chemical oscillators. They were distributed spatially in two-dimensional lattice arrangements with spacing d. Coupling among the oscillators via mass diffusion of chemicals can be varied by changing the spacing d. We used a photo-sensitive catalyst for the BZ reaction to control the reaction using light illumination. The present study addresses the onset of global synchronization with and without external noise in lattice oscillators as a function of d. We also perform numerical simulation using a modified Oregonator model.

2. Experimental setup

Chemicals and their concentrations were 0.83 M H_2SO_4, 0.28 M $KBrO_3$, 0.06 M KBr, and 0.11 M $CH_2(COOH)_2$ at room temperature of $24 \pm 1°C$. To absorb the catalyst into cation-exchange beads (50 W × 4; Muromachi Technos Co. Ltd.), beads with diameter a (0.9 ± 0.01 mm) were immersed in a ruthenium(II)–bipyridyl complex ($Ru(bpy)_3{}^{2+}$) solution controlled to the desired concentration of 2.3×10^{-5} mol/g for more than 6 h with stirring. We prepared glass boards with regular holes (0.6 ± 0.01 mm diameter) in a lattice arrangement with various lattice constants l_0 ($l_0 - a = d$) to obtain a regular lattice arrangement of beads. A bead was fixed at each hole on the board, which was then immersed into the BZ solution (20 ml) in a Petri dish. The difference of the intrinsic period of oscillation for each bead was mainly attributable to the concentration fluctuation in beads absorbing the catalyst. Oscillation was observed using a CCD camera, images of which were recorded for later analysis on a videotape and the hard disk of a computer. The time sequence of light intensity from each oscillator was obtained by averaging the gray level of the central region on the bead surface, corresponding to a grid of 8×8 pixels. A halogen lamp with intensity that was controlled by a computer was prepared to apply photic noises. Noisy light was illuminated though a 460 nm band-pass filter.

The period distribution of isolated oscillators (total: 223) was described by a unimodal distribution with an average period $T_0 = 256$ s and a standard deviation $\sigma = 7.5$ s. Analyses for each oscillator were performed from 5000 to 20 000 s after initiation of the reaction to discard the transient process to a steady state oscillation. Temporal variation of the amplitude and period of each oscillator over time were less than 10% and 5%, respectively, during the time interval.

Computer simulation was performed using the fourth-order Runge–Kutta method with the time step $\Delta t = 0.01$ s. Statistical quantities were calculated from a run of 2×10^6 time steps after discarding the initial 5×10^5 time steps as transient.

3. Results and discussion

3.1. Onset of global synchronization in the lattice

Fig. 1 shows typical examples of oscillation in a 10×10 lattice oscillator system. In large spacing, $d > 0.2$ mm, the coupling was too weak to synchronize among oscillators. All beads in the lattice oscillated in their natural frequency (Fig. 1(a)–(d)). As d decreases, beads started to synchronize with neighboring oscillators. At $d = 0.06$ mm, because of synchronization, the traveling of trigger waves was observed (Fig. 1(e)–(h)). In $d = 0.02$ mm, all nearest-neighbor beads were synchronized with one another and the trigger waves traveled all over the lattice (Fig. 1(i)–(l)). The velocity of propagating trigger waves was about 4×10^{-2} mm/s. The value of the velocity is almost identical to that in conventional excitable BZ solutions [31].

To characterize synchronization behavior in the lattice, we introduce the phase of the oscillators [32],

$$\theta_i(t) = 2\pi \frac{t - \tau_k^i}{\tau_{k+1}^i - \tau_k^i} + 2\pi k, \tag{1}$$

where τ_k^i is the time of the kth peak of the oscillatory time series of the oscillator i. The phase difference between oscillator i and j is defined as $\Delta\theta_{ij} = (\theta_i - \theta_j)\mathrm{mod}2\pi$. Fig. 2 shows the time series of the phase differences between two nearest-neighbor oscillators in a 10×10 lattice. We can distinguish the synchronization into three types: perfect synchronization, partial synchronization and no synchronization. Perfect synchronization means that no temporal development of the phase difference is observed in the two-oscillator system, as shown in Fig. 2(a). In contrast, no synchronization indicates the continuous shift of the phase difference in time, as shown in Fig. 2(c). In Fig. 2(b), both the behaviors for perfect synchronization and for no synchronization are observed for respective times. That is, the two nearest-neighbor oscillators are partially synchronized. Here, we define perfect synchronization between the nearest-neighbor oscillator i and j as the following:

$$\frac{\int_{-\delta}^{\delta} P(\Delta\theta_{ij})\,\mathrm{d}\Delta\theta_{ij}}{\int_{-\pi}^{\pi} P(\Delta\theta_{ij})\,\mathrm{d}\Delta\theta_{ij}} \geq 0.8. \tag{2}$$

In that equation, $\Delta\theta_{ij}$ indicates the phase difference between oscillator i and j. $P(\Delta\theta_{ij})$ represents the probability density of the phase difference, $\delta = 0.3\pi$, which was determined from experimental results

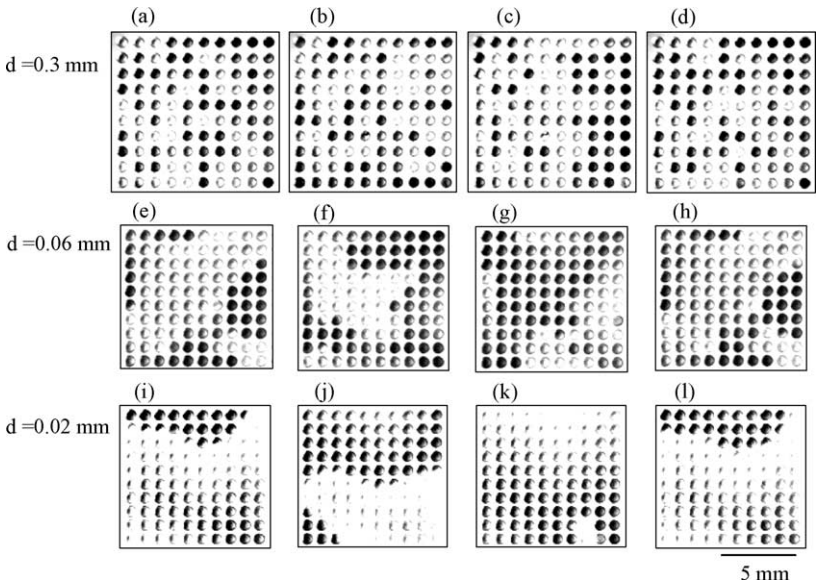

Fig. 1. Snapshots of the oscillation in a 10×10 lattice oscillator system during one period. The time interval between two images is 85 s. In (a)–(d), (e)–(h) and (i)–(l), the spacing distances d are 0.3, 0.06, and 0.02 mm, respectively. Black is in the oxidation state and white is in the reduction state.

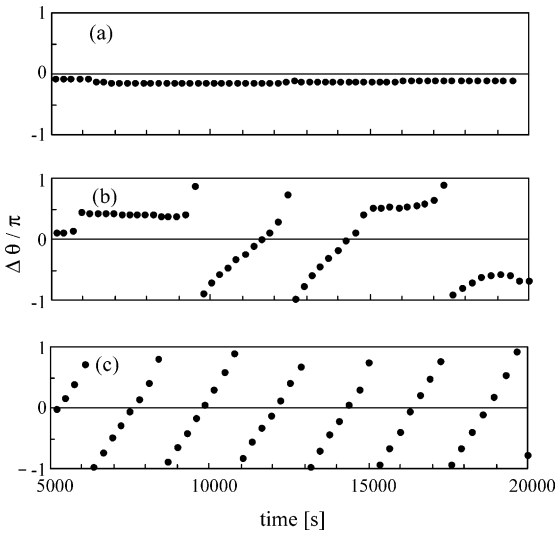

Fig. 2. Typical examples of phase differences in time between the two nearest-neighbor oscillators in a 10 × 10 lattice oscillator. (a), (b), and (c) respectively indicate perfect synchronization, partial synchronization, and no synchronization.

shown in Fig. 3. According to Eq. (1), we determined sizes of various synchronization domains (clusters). We then counted the number $N_{\max}$ of oscillators in the maximum cluster and defined an order parameter as the ratio $S = N_{\max}/N$ [4]. N is the total number of oscillators in the lattice. It is $N = 100$ in a 10×10 lattice. Fig. 4 shows the order parameter S in the 10×10 lattice as a function of d. At $d = 0.02$ mm, S is 1. As seen in Fig. 4, S decreases exponentially with increasing d, such as $S(d) = \exp(-(d - d_0)/l_S)$. The characteristic length l_S is 0.05 mm and d_0 is 0.022 mm.

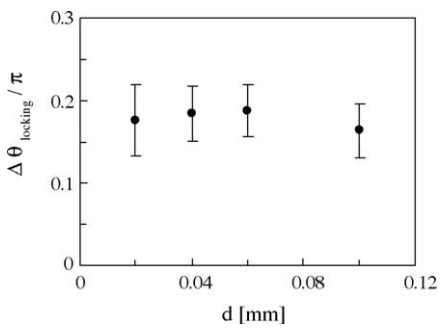

Fig. 3. The phase difference in a locking state between the two nearest-neighbor oscillators in a 10 × 10 lattice oscillator system. The error bars indicate the standard deviations.

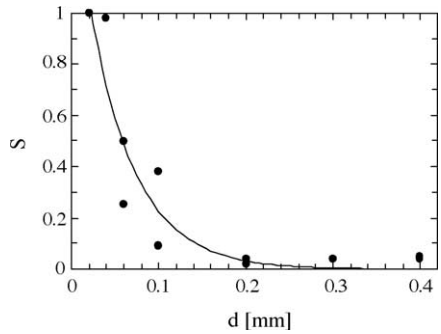

Fig. 4. Order parameter S as a function of the spacing d in a 10 × 10 lattice oscillator system. The solid line is the exponential curve $S(d) = \exp(-(d - d_0)/l_S)$.

Next, we investigate system size dependence (number of oscillators: N) because the system size may be a key characteristic scale in SDOS. The order parameter S is a good indicator if N is sufficiently large; if N is small, it is not because the resolution of S is proportional to N. Therefore, we define a new order parameter R for a small number of coupled oscillators as:

$$R = \frac{1}{n} \sum_{i,j}^{n} r_{ij}, \tag{3}$$

$$r_{ij}\, \mathrm{e}^{\mathrm{i}\Delta\Psi_{ij}} = \langle \mathrm{e}^{\mathrm{i}\Delta\theta_{ij}(t)} \rangle. \tag{4}$$

In that equation, i and j are the two nearest-neighbor oscillators; the bracket denotes the average over time [33]. The number of all combinations of nearest-neighbors is n. Fig. 5 shows the order parameter R in a 10×10 lattice (a), a 3×3 lattice (b), and a two-oscillator system (c). In Fig. 5(a), at $d = 0.02$ mm, R is 1, indicating that all oscillators are synchronized perfectly with the nearest-neighbor oscillators. R decreases exponentially with increasing d such as $R(d) = 0.45 + 0.55\ \exp(-(d - d_c)/l_R)$. It reached a constant value for $R = 0.45$, which was the statistical background due to the short time averaging for small number sampling. The characteristic length l_R is 0.048 mm, which is similar to l_S, and d_c is 0.02 mm. Thus, the dependence of R on d is similar to it of S, although they have different physical meanings: S represents the size of maximum synchronization cluster, and R represents the average of degree of synchronization between nearest-neighbor oscillators.

In Fig. 5(b), R is 1 for $d \leq 0.06$ mm. R decreases exponentially with an increase in d for $d > 0.06$ mm.

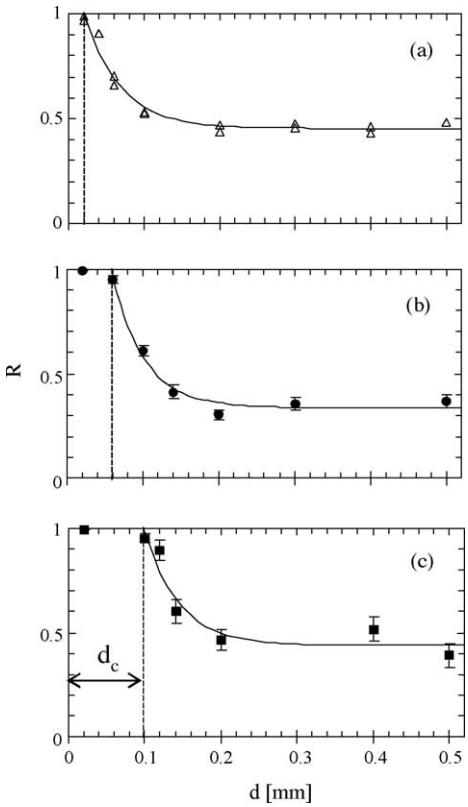

Fig. 5. Order parameter R as a function of the spacing d in a 10×10 lattice oscillator system (a), in a 3×3 lattice oscillator system (b), and in a coupled two-oscillator system (c). The solid lines are the exponential curves. The number of trials is 7–9 in (b), and 24–47 in (c). The error bars are the standard errors of R.

In Fig. 5(c), the full synchronization area d_c, which is the region with $R = 1$, is widest. Here, d_c was obtained as 0.02, 0.06 and 0.1 mm in a 10×10 lattice, in a 3×3 lattice, and in a two-oscillator system, respectively. That is, the larger the system size, the smaller the d_c.

We conducted numerical simulations using the well-known three-variable Oregonator model [34] to elucidate the exponential dependence of R on d:

$$\frac{dX_i}{dt} = k_{O1}AY_i - k_{O2}X_iY_i + k_{O3}\left(1 - \frac{Z_i}{C_{tot,i}}\right)AX_i - 2k_{O4}X_i^2 + \frac{\tilde{D}}{d^2}\sum_{\langle j\rangle}(X_j - X_i), \quad (5)$$

$$\frac{dY_i}{dt} = -k_{O1}AY_i - k_{O2}X_iY_i + hk_{O5}MZ_i + \frac{\tilde{D}}{d^2}\sum_{\langle j\rangle}(Y_j - Y_i), \quad (6)$$

$$\frac{dZ_i}{dt} = 2k_{O3}\left(1 - \frac{Z_i}{C_{tot,i}}\right)AX_i - k_{O5}MZ_i. \quad (7)$$

Here, X_i, Y_i, and Z_i are the concentrations of $HBrO_2$ (activator), Br^- (inhibitor) and oxidized catalyst $Ru(bpy)_3{}^{3+}$ in oscillator i, respectively: $A = [BrO_3{}^-]$; $M = [\text{malonic acid}]$; h is the stoichiometric factor; and $k_{O1} - k_{O5}$ are the rate constants. The total catalyst ions ($[Ru(bpy)_3{}^{2+}] + [Ru(bpy)_3{}^{3+}]$) are $C_{tot,i}$ in the oscillator i, which determines a natural period of oscillator i. The period distribution of individual oscillators is given by the Gaussian distribution with an average period T_0 and a standard deviation $\sigma/T_0 = 0.05$. Because the catalyst ions are fixed on the beads, coupling among oscillators is mediated only by diffusions of both X and Y with the coupling strength $\tilde{D}/d^2$, where $\tilde{D}$ is the effective diffusion constant. $\sum_{\langle j\rangle}$ indicates the summation over the nearest-neighbors of the oscillator i. Therefore, the coupling is local.

Fig. 6 shows the numerical result for order parameter R as a function of d. As was already shown in the experiment, the values of R decrease exponentially with increasing d. That is, the exponential dependence of R on d can be described by the local coupling model. However, the specific aspect of d_c observed in Fig. 5 is not obtained in our numerical simulation. It is probably attributable to the missing necessary characteristic lengths. Further study will be necessary to address this point.

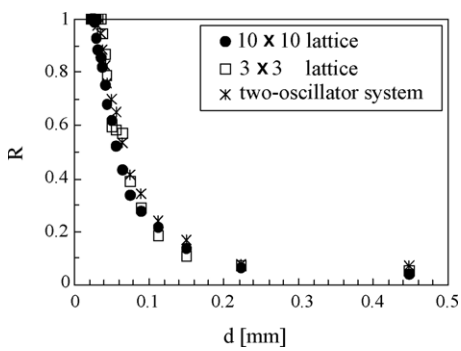

Fig. 6. R as a function of d obtained from numerical calculation. The parameter values are $A = 0.15\,M$, $M = 0.2\,M$, $\tilde{D} = 4 \times 10^{-8}\,cm^2\,s^{-1}$, $k_{O1} = 2H^2\,M^{-3}\,s^{-1}$, $k_{O2} = 3 \times 10^6 H\,M^{-2}\,s^{-1}$, $k_{O3} = 42H\,M^{-2}\,s^{-1}$, $k_{O4} = 3 \times 10^3\,M^{-1}\,s^{-1}$, and $k_{O5} = 5\,M^{-1}\,s^{-1}$, where $H = 0.37\,M$.

3.2. Noise-induced synchronization

Constant light illumination suppresses oxidation through photochemical production of Br^-, an inhibitor of autocatalysis in the BZ reaction. As light intensity increases, the period of the oscillation increases and suddenly stops at a threshold intensity of $I_{th} \sim 3.2\,mW/cm^2$.

Next we investigate the role of external noise in SDOS using a noisy light source. Noises were superimposed with a constant and noisy light as $I = I_{DC} + I_N\xi(\delta t)$, where I_{DC} was the constant light intensity, I_N the amplitude of the noise, and $\xi(\delta t)$ a random variable in time equally distributed between -1 and 1. $\xi(\delta t)$ was generated by a computer using a program for random digit production; δt was the interval of random pulses. In the present study, $\delta t = 30$ s. The constant light intensity I_{DC} was $3.0\,mW/cm^2$ for maintaining the system slightly below the threshold—a subthreshold state.

Fig. 7 shows the order parameter R as a function of the noise intensity I_N for the 10×10 lattice oscillators with $d = 0.06$ mm. R shows the maximum at an optimal noise intensity. Thereby, noise-induced synchronization in SDOS in BZ reaction can be observed experimentally. The optimal noise intensity I_N^* is about $0.3\,mW/cm^2$. Noises may play an important role in synchronization, such as modifying the characteristic length and/or coupling strength. More details to elucidate this role are being sought in separate studies.

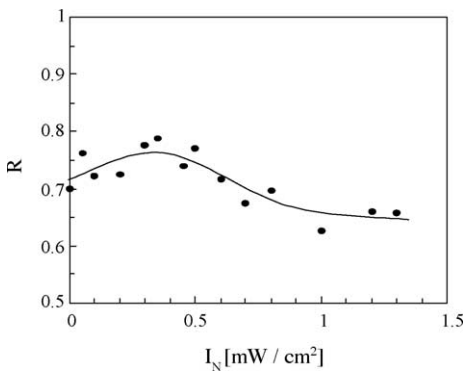

Fig. 7. Order parameter R as a function of noise intensity I_N in a 10×10 lattice oscillator system.

4. Summary and conclusion

We used experimentation to study global synchronization in two-dimensional lattices of discrete BZ oscillators. When the coupling strength increased, i.e. decreasing the spacing d between two beads, synchronization clusters of oscillators emerged and grew into the whole system. Two order parameters, R and S, were defined and employed based on synchronization in pairs of nearest-neighbor oscillators, which can well describe the synchronization state. R and S depend on d exponentially. The same characteristic length for both is observed. The critical distance d_c depends on the total number of oscillators, i.e. the system size. However, exponential curves (characteristic slopes) for $R(d)$ do not depend on the system size. Noise synchronization is observed. That is, the maximum R is observed at an optimal noise intensity. Non-locality of the coupling has not been addressed in present study, but it is possible for careful choice of the concentrations and system sizes. Probably, the present lattice (10×10) is not sufficiently large to realize a non-local oscillator system. More details regarding synchronization dynamics are now in progress.

Acknowledgements

We are grateful to Prof. H. Sakaguchi of Kyushu University for helpful discussion. This work was supported in part by a Research Fellowship of the Japan Society for the Promotion of Science for Young Scientists (No. 0307712). This paper is dedicated to Prof. Kuramoto who has retired in this year from Kyoto University. One of author (SK) has been continuously encouraged from Prof. Kuramoto to work in dissipative structures and nonlinear dynamics for more than 30 years with kind friendship.

References

[1] A. Pikovsky, M. Rosenblum, J. Kurths, Synchronization: A universal concept in nonlinear science Cambridge University Press, Cambridge, 2001.
[2] Y. Kuramoto, Chemical Oscillations, Waves and Turbulence, Springer-Verlag, Berlin, 1984.
[3] H. Daido, Physica D 91 (1996) 24.

[4] H. Sakaguchi, S. Shinomoto, Y. Kuramoto, Prog. Theor. Phys. 77 (1987) 1005.
[5] T. Aoyagi, Y. Kuramoto, Phys. Lett. A 155 (1991) 410.
[6] M. Bahiana, M.S.O. Massunaga, Phys. Rev. E 49 (1994) R3558.
[7] H. Daido, Phys. Rev. Lett. 61 (1988) 231.
[8] P. Östborn, S. Åbeg, G. Ohlén, Phys. Rev. E 68 (2003) 015104.
[9] K. Satoh, J. Phys. Soc. Jpn. 58 (1989) 2010.
[10] H. Sakaguchi, S. Shinomoto, Y. Kuramoto, Prog. Theor. Phys. 79 (1988) 1069.
[11] K. Wiesenfeld, P. Colet, S.H. Strogatz, Phys. Rev. Lett. 76 (1996) 404.
[12] R.A. Oliva, S.H. Strogatz, Int. J. Bifurc. Chaos 11 (2001) 2359.
[13] I.Z. Kiss, Y. Zhai, J.L. Hudson, Science 296 (2002) 1676.
[14] K. Miyakawa, K. Yamada, Physica D 151 (2001) 217.
[15] Z. Néda, E. Ravasz, Y. Brechet, T. Vicsek, A.-L. Barabási, Nature 403 (2000) 849.
[16] R. Segev, M. Benveniste, E. Hulata, N. Cohen, A. Palevski, E. Kapon, Y. Shapira, E. Ben-Jacob, Phy. Rev. Lett. 88 (2002) 118102.
[17] A.N. Zaikin, A.M. Zhabotinsky, Nature 225 (1970) 535.
[18] A.T. Winfree, Science 175 (1972) 634.
[19] K.I. Agladze, V.I. Krinsky, Nature 296 (1982) 424.
[20] J. Maselko, J.S. Reckley, K. Showalter, J. Phys. Chem. 93 (1989) 2774.
[21] N. Nishiyama, K. Eto, J. Chem. Phys. 100 (1994) 6977.
[22] N. Nishiyama, Physica D 80 (1995) 181.
[23] N. Nishiyama, T. Matsuyama, J. Chem. Phys. 106 (1997) 3427.
[24] K. Miyakawa, T. Okabe, M. Mizoguchi, F. Sakamoto, J. Chem. Phys. 103 (1995) 9621.
[25] K. Fujii, D. Hayashi, O. Inomoto, S. Kai, Forma 15 (2000) 219.
[26] H. Fukuda, H. Nagano, S. Kai, J. Phys. Soc. Jpn. 72 (2003) 487.
[27] Y. Kuramoto, S.J. Hogan, et al. (Eds.), Nonlinear Dynamics and Chaos. Where do we go from here? IOP Publishing Ltd., 2003, p. 209.
[28] Y. Kuramoto, Prog. Theor. Phys. 94 (1995) 321.
[29] D. Tanaka, Y. Kuramoto, Phys. Rev. E 68 (2003) 026219.
[30] S. Shima, Y. Kuramoto, Phys. Rev. E 69 (2004) 036213.
[31] S.K. Scott, Oscillations, Waves, and Chaos in Chemical Kinetics, Oxford University Press, 1994.
[32] C. Zhou, J. Kurths, B. Hu, Phys. Rev. Lett. 87 (2001) 098101.
[33] A.B. Neiman, D.F. Russell, Phys. Rev. Lett. 88 (2002) 138103.
[34] A.L. Kawczyński, W.S. Comstock, R.J. Field, Physica D 54 (1992) 220.